Purdue University

Purdue e-Pubs

Department of Electrical and Computer Engineering Technical Reports

Department of Electrical and Computer Engineering

10-1-1985

Analysis of Robot Drive Train Errors and Their Compensation

Shaheen Ahmad
Purdue University

Follow this and additional works at: https://docs.lib.purdue.edu/ecetr

Ahmad, Shaheen, "Analysis of Robot Drive Train Errors and Their Compensation" (1985). *Department of Electrical and Computer Engineering Technical Reports.* Paper 549.
https://docs.lib.purdue.edu/ecetr/549
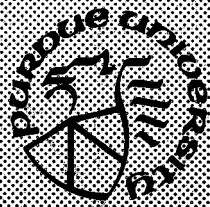
Analysis of Robot Drive Train Errors and Their Compensation

Shaheen Ahmad

School of Electrical Engineering
Purdue University
West Lafayette, Indiana 47907

ANALYSIS OF ROBOT DRIVE TRAIN
ERRORS AND THEIR COMPENSATION

Shaheen Ahmad
School of Electrical Engineering
Purdue University
West Lafayette, IN 47907
U.S.A.

Abstract

This paper presents a mathematical model of the kinematic nonlinear drive train errors which reduce absolute static positioning accuracy of robot arms. This kinematic inaccuracy renders robot manipulators ineffective when programmed off-line, though they might be programmed to successfully perform the same task by "Teach Play back" schemes. The kinematic drive train inaccuracy model, presented in this paper can be used to predict and compensate for these second order effects on-line, without resorting to sensor based programming techniques, which are often expensive and difficult to implement in an industrial environment.

The drive train error model presented in this paper is based on gear backlash, eccentricity and drive shaft compliance.

Introduction

Robot arms have been traditionally used in pick and place type assembly operations, where the arms repeatability and resolution have been two key issues. Modern robots are often programmed by "Teach Playback Schemes", where the human operator ensures the end effector reaches the work point by closing the sensing loop, see Fig. 1. However, as the 'teach playback' schemes require the robot and other plant equipment to be set up, prior to program development, new programming techniques are being adopted by the industry. These include off-line programming via high level languages such as VAL-II [Shimano et al. 84], AML [Taylor et al. 83], etc, also via simulated teach by doing on CAD (Computer Aided Design) work stations. Although these programming techniques are not new and have been in used research environment in the past, they have focused on a new problem involving the absolute positioning accuracy of the robot arm.

This paper presents a mathematical model of the nonlinear kinematic drive train effects which limits the absolute steady state positioning capability of the robot arm. The absolute positioning capability is limited by the following sources (effects due to control system design are not discussed in this paper):

(i) Link parameter errors,

(ii) Backlash, or lost motion,

(iii) Nonlinearity in the drive train transmission,

(iv) Compliance of each link joint,

(v) Feedback quantisation.

The first part of this paper deals with the link parameter errors, and its effects on the end effector position. The second part of the paper models the effect of backlash in the joint drive and illustrates how it may be compensated. The gear eccentricity effects are discussed in section three. Section four outlines how joint compliance effect can also influence end effector positioning accuracy. The final section outlines the positioning accuracy limitations of the manipulator as imposed by quantisation of the position feedback signal.

1. Link Parameter Error

The kinematic model of the manipulator is obtained by modeling each linkage by a (4 x 4) transformation, the homogeneous transform [Paul 81]. The Fig. 2 shows the link parameters which make up the homogeneous transform. It consists of the twist angle 'α', link length 'a', link offset length 'd' and the joint angle 'θ'. The homogeneous link transform is thus given as:

$$T_i^2 = \text{Rot }(Z,\theta) \text{ trans }(0,0,d) \text{ trans }(0,0,a) \text{ Rot }(X,\alpha) \qquad (1)$$

The motion of the end effector with respect to the manipulator base frame is given by T_0^6, which is obtained by the product of the individual link transforms:

$$T_0^6 = \prod_{i=0}^{5} T_i^{i+1} \qquad (2)$$

However, if any of the link parameters are inexact, such as the link lengths:

$$a \rightarrow a + da \qquad (3)$$

Then, the end effector is displaced by dT_0^6, such that:

$$dT_o^6 + T_o^6 = \prod_{i=0}^{5} T_i^{i+1} (I + dT_i) \qquad (4)$$

The end effector transform error, dT_o^6, can be physically measured, as the link length error causes the end effector to be displaced from the demanded position. Altering link length does not result in an orientation error.

As most industrial robot arms are made of cast linkages with machined link joints, manufacturing tolerances introduce errors in link parameters i.e:

$$a \rightarrow a + da$$
$$d \rightarrow d + \delta$$
$$\alpha \rightarrow \alpha + d\alpha \qquad (5)$$

Castings typically shrink when they are cooled; in addition, thermal effects can also lead to variation in joint lengths e.g:

$$a(T) = a_o (1 + \mu (T - T_o)) \qquad (6)$$

where μ is the thermal expansion coefficient, T_o and T are nominal and actual temperatures, given the nominal length is a_o. Similar expansions is also valid for other link parameters.

Problem is to improve manipulator accuracy by obtaining an estimate of the (n x 1) vector of link length error, da, (n x 1) vector of δ and (n x 1) vector of twist angle errors $d\alpha$. Hayati and Wu [Hayati 83] [Wu 83] have shown that a linear error model can be found between observed cartesian error dx and the link parameter errors $[da, \delta, d\alpha]^t$.

$$dx = J_\alpha \, d\alpha + J_a \, da + J_\delta \, \delta + J_\theta \, d\theta. \qquad (7)$$

where J_α is (6 x n) matrix relating cartesian errors with twist angle error. Similar relations between (J_a, da), $(J$ and $\delta)$ exists. Note that an error in $d\theta$ is transformed to the cartesian frame by the usual manipulator Jacobian J_θ.

Details of how to evaluate $(J_\alpha, J_a, J_\delta)$ can be found in previous analysis on link parameters errors [Hayati 83] [Wu 83].

By calibrating the manipulator to a number of positions and recording its error, an estimate of parameter error, $\hat{\Phi} = [da, \delta, d\alpha]^t$, may be obtained by least square error techniques. Whitney [Whitney et al. 84] has carried out positioning (without orientation) calibration of the first three degrees of freedom of the PUMA 560 (Fig. 3) arm. Whitney shows that such calibration can increase the positioning accuracy by a factor

of 10, from 3mm to 0.3mm.

Equally important as the parameter errors, Φ, is the error in the relative angle between the joints, $d\theta$. The next section outlines their sources and error models.

2. Errors In Joint Angle $d\theta$ Due to Backlash

Backlash effects are mainly observed due to the fact that joint sensors are located on the actuator rather than on the joint see, Fig. 4. As a result, gear train backlash and nonlinear effects are not sensed, thus causing an error, $d\theta$. In this section the backlash error, $d\theta$, that propagates through the drive train is modeled.

The Fig. 5 illustrates a backlash gap, which causes the output motion not to directly follow the input motion. The relationship between the input and output motion for one set of gears may be represented by the graph in Fig. 6. The output begins to follow the input once the parts are in contact (see Fig. 5), hence output motion of $(i+1)^{th}$ gear can be modeled in terms of motion of ith gear as:

$$\theta_{i+1} = (\theta_i - C_i^{\pm} \, d\theta_i^b) \, \frac{n_{gi+1}}{n_{gi}} \qquad (8)$$

where θ_{i+1} = Angular displacement of $(i+1)^{th}$ gear

$\quad \theta_i$ = Angular displacement of (i^{th}) gear

$\quad d\theta_i^b$ = Backlash in i, $(i+1)^{th}$ gear contact

$\quad n_{gi+1}$ = Number of gear teeth on $(i+1)^{th}$ gear

$\quad n_{gi}$ = Number of gear teeth on i^{th} gear

The gear contact is modeled by the coefficient $C^{\pm}$, which assumes a value of 1 or 0, hence:

$$C_i^{\pm} = \begin{cases} +1 & ; \quad C^- \text{ gears not in contact.} \\ 0 & ; \quad C^+ \text{ gears are in contact.} \end{cases} \qquad (9)$$

A reduction ratio, K_{gi+1}, is given as:

$$K_{gi+1} = \left(\frac{n_{gi}}{n_{gi+1}} \right) \qquad (10)$$

Usually, $K_{gi+1} < 1$, as the actuator is required to drive a larger load. If the gear, corresponding to i=0, is the motor shaft rotation θ_m, then output motion of the

gearbox which causes joint motion, θ_{arm}, is given as:

$$\theta_{arm} = \theta_m \prod_{i=1}^{n} K_{gi} - \sum_{i=1}^{n} C_i^{\pm} d\theta_i^b \prod_{r=1}^{i} K_{gr} \qquad (11)$$

This corresponds to the joint motion due to an 'n' gear train. If all the gear pair backlash gaps are almost equal and a reduction ratio ($K_{gi} < 1$) exists for all gear pairs, then:

$$\text{iff } [d\theta_i^b = d\theta^b : i = 1 \ldots n]$$

$$\text{and iff } [K_{gi} < 1 : i = \ldots n] \qquad (12)$$

Then, only the last term in equation (11) is most significant. Assuming n_{gnom} (>1) is the nominal reduction ratio in the joint gear train, then:

$$\theta_{arm} \cong \frac{1}{n_{gnom}} \theta_m - C_n^{\pm} K_{gn} d\theta^b \qquad (13)$$

If there is an external load on the arm, such as the gravitational force due to the arm's weight, the backlash is taken up when upward motions are executed (e.g. the backlash of PUMA's link 2 and 3) ,then $C^+ = 0$. In downward motion the backlash has to be overcome, i.e. $C^- = 1$. The PUMA base joint is not preloaded by gravity, and $C^{\pm}$ has to be constantly updated if forward motion is executed without any reversal of the motor shaft. Then ,the gear's are in contact, i.e. $C^+ = 0$.

Backlash Compensation

The backlash may now be compensated on-line by altering the demand signal to the motor as:

$$\theta_m = n_{gnom} [\theta_{arm} + C_n^{\pm} K_{gn} d\theta^b] \qquad (14)$$

3. Errors in Joint Angle Due to Variation
In Reduction Ratio

One other problem which effects the positioning accuracy of the joint is the gear eccentricity. Machined gears tend to be elliptical, and a very small variation in the dimensions between the axes exist, see Fig. 7. The input gear will usually have a much smaller variation in dimensions than the output gear, if a reduction ratio exists. As a result the smaller drive gear can be assumed to be near perfectly round, of radius r_o (see Fig. 7). The larger gear has a radius which varies from r_{gnom} to r_{gmax}. As the gear turns through an angle θ_g, the radius of the contact point is given as :

$$r_g(\theta) = r_{gnom} (1 + \epsilon_g \, Sin \, \theta_g) \tag{15}$$

$$where \; \epsilon_g = \left(\frac{r_{gmax} - r_{gnom}}{r_{gnom}} \right) \tag{16}$$

usually the eccentricity is small, $\epsilon_g < 10^{-3}$. The reduction ratio is then given as:

$$n_g(\theta) = \frac{r_o}{r_g(\theta)} = \frac{1}{n_{gnom}(1 + \epsilon_g \, Sin \, \theta_g)} \tag{17}$$

$$where \; n_{gnom} = \left(\frac{r_o}{r_{gnom}} \right) \tag{18}$$

and n_{gnom} is the ideal gear ratio. As $n_{gnom} > 1$, for any joint, the final gear pair will have the most significant effect in terms of the variation of the reduction ratio with respect gear angle θ_g :

$$n_g(\theta) = \frac{1}{n_{gnom}} \cdot \prod_{i=1}^{n} \frac{1}{[1 + \epsilon_i \, Sin \, \theta_{gi}]} \tag{19}$$

Variation of reduction ratio with respect to two gears in the drive train is given in Fig. 8.

Drive Train Gear Eccentricity Error Compensation

The motor demand may now be altered to overcome this transmission error due to drive train eccentricity:

$$\theta_m = \frac{1}{n_g(\theta)} [\theta_{arm} + C_n^{\pm} K_{gn} \, d\theta_n^b] \tag{20}$$

$$\theta_m = n_{gnom} [\theta_{arm} + C_n^{\pm} K_{gn} \, d\theta_n^b] (\prod_{i=1}^{n} [1 + \epsilon_j \, Sin \, \theta_{gj}]) \tag{20}$$

If second order terms involving $\epsilon_i \epsilon_j < 10^{-6}$ are ignored, then:

$$\prod_{i=1}^{n} [1 + \epsilon_i \, Sin \, \theta_{gi}] \cong 1 + \sum_{j=1}^{n} (\epsilon_j \, Sin \, \theta_{gj}) \tag{21}$$

$$\theta_m \cong n_{gnom} [\theta_{arm} + C_n^{\pm} Kg_n \, d\theta_n^b] [1 + \sum_{i=1}^{n} \epsilon_i \, Sin \, \theta_{gi}] \tag{22}$$

This will effectively compensate for the variation in the reduction ratio. The phase angle of the ith gear is given in term of its original position θ_{gi}^o and the gear ratio K_{gi}:

$$\theta_{gi} = K_{gi} \left[d\theta_{gi-1} - C_{i-1}^{\pm} \, d\theta_{i-1}^{b} \right] + \theta_{gi}^{o} \qquad (23)$$

where θ_{gi} is the new angular position of the ith gear if $(i-1)^{th}$ shaft is turned through an angle $d\theta_{gi-1}$. The position of the ith shaft is related to the motor shaft motion $d\theta_{m}$ as:

$$\theta_{gi} = \left\{ \prod_{\ell=0}^{i} K_{g_{\ell}} \right\} d\theta_{m} - \sum_{r=1}^{i} C_{r}^{\pm} \, d\theta_{r}^{b} \prod_{p=1}^{r} K_{gp} + \theta_{gi}^{o} \qquad (24)$$

The angle θ_{gi}^{o} is the initial phase angle prior to any motion. Thus, it is possible to track the value of the summation term in equation (22), in which the most significant term is likely to be due to the last reduction pair, as 'ϵ' is usually the largest for the final joint. The PUMA, for example, has a 'Bull gear' of significantly large diameter on the final drive of the elbow, shoulder and the base joint (see Fig. 9). In such a circumstance, a simplification may be made, i.e:

$$\text{iff } \epsilon_{n} \gg \epsilon_{j} : j = 1 \, .. \, (n - 1), \text{ then:}$$

$$\sum_{j=1}^{n} \epsilon_{j} \, \text{Sin} \, \theta_{gi} \cong \epsilon_{n} \, \text{Sin} \, \theta_{gn}$$

$$\cong \epsilon_{n} \, \text{Sin} \left[\frac{1}{n_{gnom}} \cdot d\theta_{m} - C_{n}^{\pm} K_{gn} \, d\theta^{b} + \Phi \right] = \epsilon_{n} \, \text{Sin} \left[\frac{1}{n_{gnom}} \, d\theta_{m} + \phi^{*} \right] \qquad (25)$$

where Φ^{*}, and Φ are the phase advances in the drive with and without backlash respectively.

4. Positioning Errors Due to Joint Compliance

Currently, most industrial robots have compliant joints. This is apparent when a large load is handled, the arm is then seen to deflect, resulting in end effector positioning error. The joint compliance results from the torsional stiffness of the gearbox and the output drive shaft actuating the joint. If the joint deflection due to the mass of the arm and the carried workpiece can be estimated, then compensation can be made to correct the static positioning error. The problem is then to estimate what is the steady state positioning error, when a constant load, equivalent to the workpiece mass is applied at the end effector. If the carried workpiece has mass 'mg' Newtons, then the force seen with respect to the base frame of the manipulator is ^{B}F:

$$\mathbf{^B F} = \begin{bmatrix} 0 \\ 0 \\ -mg \\ 0 \\ 0 \\ 0 \end{bmatrix} \tag{27}$$

The load torque seen at the joints in the steady state due to the workpiece is $\tau = (\tau_1, \ldots, \tau_n)^t$:

$$\tau = \begin{bmatrix} ^{EB}_{q} J \end{bmatrix}^t {^B F} \tag{28}$$

where, $^{EB}_{q} J$ is the Jacobian relating differential motion of the end effector frame E, aligned to the base frame B, and the joint frame q (See Fig. 10).

During static positioning, when this additional load τ is applied, the resulting motion has velocities and acceleration terms close to zero. As a result, the motions may be independently studied for each joint (dynamic effects can be ignored). The simplified model of each joint and its equivalent compliant members is illustrated in Fig. 11 (A more realistic drive train model and its analysis is given in the Appendix). The equation of motion of the joint motor shaft θ_m is given by:

$$T_m = J_m \ddot{\theta}_m + B_m \dot{\theta}_m + f_{cms} + T_1 \tag{29}$$

where T_m is the motor torque, J_m is the effective motor inertia, and B_m is the effective motor viscous friction. The coulomb - static friction term, f_{cms}, is given as:

$$f_{cms} = \begin{cases} + \mid f^m_{static} \mid & ; \text{ if } \dot{\theta}_m = 0 \\ \text{sgn}\,(\dot{\theta}_m) \mid f^m_{Coulomb} \mid & ; \text{ if } \mid \dot{\theta}_m \mid \neq 0 \end{cases} \tag{30}$$

The torque T_1 in equation (29) is the reaction torque exerted at the motor shaft due to the external load and the drive train. If the effective compliance of the gearbox is reflected to the joint drive shaft, then the motion of the final gear is given as:

$$T_2 = J_g \ddot{\theta}_g + B_g \dot{\theta}_g + f_{cmgs} + K_s (\theta_g - \theta_{arm}) \tag{31}$$

where K_s is the effective drive train joint compliance. The motion of the arm θ_{arm} is given as:

$$T_d = J_{arm} \ddot{\theta}_{arm} + K_s (\theta_{arm} - \theta_g) \tag{32}$$

where T_d is the load torque applied to the arm. The motion of the gear train and the motor shaft are related by:

$$\theta_g = \frac{1}{n_a} \theta_m \tag{33}$$

$$T_2 = n_a T_1 \tag{34}$$

where 'n_a' is the amplification ratio between the motor and gear torques, i.e. ($n_a > 1$). The equation of motion of the motor shaft angle θ_m is further simplified as:

$$T_m = \left[J_m + \frac{J_g}{n_a^2}\right] \ddot{\theta}_m + \left[B_m + \frac{B_g}{n_a^2}\right] \dot{\theta}_m + f_{cmgs}$$

$$+ \frac{K_s}{n_a} \left[\frac{\theta_m}{n_a} - \theta_{arm}\right] \tag{35}$$

and

$$f_{cmgs} = \begin{cases} |f_{static}^m| + \frac{1}{n_a} |f_{static}^g| & ; \text{if } \dot{\theta}_m = 0 \\[2mm] \text{sgn}(\dot{\theta}_m)\{ |f_{Coulomb}^m| + (\frac{+1}{n_a})|f_{Coulomb}^g| \} & ; \text{if } |\dot{\theta}_m| \neq 0 \end{cases}$$

$$\tag{36}$$

The motor shaft position, $\theta_m(s)$, is obtained as:

$$\theta_m(s) = \frac{\left[\dfrac{K_s n_a T_d(s)}{n_a^2(J_{arm} s^2 + K_s)} + T_m(s) - f_{cmgs}(s)\right]}{\left\{\left[J_m + \dfrac{J_g}{n_a^2}\right]s^2 + \left[B_m + \dfrac{B_g}{n_a^2}\right]s + \dfrac{K_s}{n_a^2} - \dfrac{K_s^2}{n_a^2(J_{arm} s^2 + K_s)}\right\}}$$

$$\tag{37}$$

The steady state value of the motor shaft position, θ_{ss}^m, is given by the final value theorem as:

$$\theta_{ss}^m = \text{Lim}_{s \to 0} \{s \, \theta_m(s)\} \tag{38}$$

In the static situation, the friction and external loads are constant:

$$T_d(s) = \frac{T_d}{s} \tag{39}$$

$$f_{cmgs}(s) = \frac{f_{cmgs}}{s} \tag{40}$$

Figure 11 depicts the control problem in which the robot controller demands a torque $T_m(s)$ to overcome the load (motor dynamics are ignored, and a torque servo is assumed):

$$T_m(s) = G_c(s) \left[\frac{n_a}{s} \theta_{arm}^d - \theta_m(s) \right] \tag{41}$$

where θ_{arm}^d is the joint goal position, and the controller transfer function is given by $G_c(s)$. The torque $T_m(s)$ will obviously vary with the controller structure $G_c(s)$; hence, the steady state motor position. Table 1 below lists the steady state motor position, θ_m^{ss}, and the steady state arm position, θ_{arm}^{ss}, which is given by:

$$\theta_{arm}^{ss} = \mathcal{L}imit_{s \to o} \, s \left\{ \frac{n_a \, T_d(s) + K_s \, \theta_m(s)}{n_a \, (J_{arm} \, s^2 + K_s)} \right\} \tag{42}$$

The steady state motor position error, $d\theta_m^{ss}$, is given by:

$$d\theta_m^{ss} = n_a \, \theta_{arm}^d - \theta_m^{ss} \tag{43}$$

Similarly, the steady state arm position error, $d\theta_{arm}^{ss}$, is:

$$d\theta_{arm}^{ss} = \theta_{arm}^d - \theta_{arm}^{ss} \tag{44}$$

It is seen from table 1 that the proportional (P), proportional and derivation (PD), type zero controller have the same performance. The PID (proportional integral and derivative) controller has the best performance $d\theta_m^{ss} = 0$ (as expected). However, the arm position error is given as:

$$d\theta_{arm,PID}^{ss} = - \frac{T_d}{K_s} \tag{45}$$

This is equivalent to a load T_d applied to one end of a torsional spring which has the other end permanently fixed (equivalent to $T_m = \infty$). Indeed, one intuitively expects the arm to act as, 'nothing but a torsional spring', in the steady state.

Joint Deflection Error Compensation

The actual arm set point, θ_{arm}, must be altered by $d\theta_{arm}^{ss}$ in order to compensate for the joint deflection:

$$\theta_{arm}^{altered} = \theta_{arm}^d - d\theta_{arm}^{ss} \tag{46}$$

If a load of '-mg' is applied, the arm will be displaced by '$+d\theta_{arm}^{ss}$' and the new set

point will correct the end effector position. The compensated motor demand position, θ_m, is then given as:

$$\theta_m \cong n_{gnom} \left[\theta_{arm}^d - d\theta_{arm}^{ss} + C_n^{\pm} K g_n \, d\theta_n^b \right] \left[1 + \epsilon_n \sin\left(\frac{1}{n_{gnom}} \cdot d\theta_m + \Phi^* \right) \right] \qquad (47)$$

G(s) Controller Structure	θ_m^{ss}	$d\theta_m^{ss}$	θ_{arm}^{ss}	$d\theta_{arm}^{ss}$
K_p	$n_a \theta_{arm}^d - \frac{1}{K_p}(f_{cmp} - \frac{T_d}{n_a})$	$\frac{1}{K_p}(f_{cmp} - \frac{T_d}{n_a})$	$\theta_{arm}^d + \frac{T_d}{K_s} + \frac{1}{n_a K_p}(\frac{T_d}{n_a} - f_{cmp})$	$K e_i - \frac{T_d}{K_s} - \frac{1}{n_a K_p}(\frac{T_d}{n_a} - f_{cmp})$
$K_p + SK_D$	$n_a \theta_{arm}^d - \frac{1}{K_p}(f_{cmp} - \frac{T_d}{n_a})$	$\frac{1}{K_p}(f_{cmp} - \frac{T_d}{n_a})$	$\theta_{arm}^d + \frac{T_d}{K_s} + \frac{1}{n_a K_p}(\frac{T_d}{n_a} - f_{cmp})$	$-\frac{T_d}{n_a} - \frac{1}{n_a K_p}(\frac{T_d}{n_a} - f_{cmp})$
$K_p + SK_D + \frac{K_I}{S}$	$n_a \theta_{arm}^d$	0	$(\frac{T_d}{K_s} + \theta_{arm}^d)$	$-(\frac{T_d}{K_s})$

Table 1
Steady State Positioning Error Due to Controller
Performance and Joint Compliance.

5. Limitation on the Absolute Positioning Accuracy

The discrete nature of joint feedback signals impose a limitation on the absolute positioning accuracy of the manipulator. This limitation is easily determined if the effective joint angular resolution α_{rmin} is first determined. If K_{ei} is the ith joint feedback resolution per revolution, then α_{rmin}^i is:

$$\alpha_{rmin}^i = \frac{2\pi}{[n_{ai} K_{ei}]} \qquad (48)$$

where n_{ai} ($= n_{gnom}^i$) is the ith joint gear ratio. The overall angular resolution of the n-jointed robot is then:

$$\alpha_{rmin} = \max \{\alpha_{rmin}^i : i = 1 \ldots n \}$$

$$= \frac{2\pi}{[\min \{ (n_{ai} K_{ei}) : i = 1 \ldots n \}]} \qquad (49)$$

An (n x n) diagonal matrix $[e_s]$ can then be defined. It converts a unit feedback signal into α_{rmin}^i units:

$$[e_s] = \text{diag}(\alpha_{rmin}^i)$$

$$= \alpha_{rmin} \; diag \; (\frac{\alpha_{rmin}^i}{\alpha_{rmin}})$$

$$= \alpha_{rmin} \; [e_{sc}] \tag{50}$$

If the (n x 1) joint position demand vector, in feedback units, is $e_{dmd} = [e_1, \ldots, e_n]^t$, then a unit demand in position change (in feedback units) $\hat{e}_{dmd} = [1, \ldots, 1]^t$, corresponds to the minimum angular displacement $d\theta_{min}$:

$$d\underset{\sim}{\theta}_{min} = \alpha_{rmin} \; [e_{sc}] \; \hat{e}_{dmd} \tag{51}$$

The corresponding change in the end effector in base coordinates is given as:

$$d\underset{\sim}{X}_q = \alpha_{rmin} \; _q^B J \; [e_{sc}] \; \hat{e}_{dmd} \tag{52}$$

where $d\underset{\sim}{X}_q$ corresponds to the minimum displacement the end effector is capable of making about any arm posture $\underset{\sim}{\theta} = [\theta_1 \ldots, \theta_n]^t$. Theoretically, it should be possible to position the manipulator tool at the vertices of the quantisation cube $d\underset{\sim}{X}_q$ (see Figure 12). The quantisation cube is dependent on the manipulator jacobian, hence the arm posture $\underset{\sim}{\theta}$.

6. Conclusion

A model of the non-linear drive train errors has been presented in this paper. The errors have included effects due to gear backlash, eccentricity and gear-drive shaft compliance. The static joint positioning errors due to these effects, also their compensation have been proposed in this paper. Absolute accuracy limitation of the manipulator, based on kinematics and feedback quantisation has also been outlined. It would, however, be necessary to look at the manipulator dynamical effects [Yoshikawa 85] and the controller structure, in order to predict realistic positioning accuracy limitation of a robot arm. Dynamical positioning accuracy of the manipulator due to the drive train non-linear effects and their compensation is being currently investigated.

References

[Hayati 83] Hayati S., "Robot Arm Geometric Link Parameter Estimation", Proceedings of the 22nd IEEE Conference on Decision and Control, 1477-1483, December 1983.

[Paul 81] Paul R.P., "Robot Manipulators: Mathematics, Programming and Control", MIT Press 1982.

[Shimano et al. 84] Shimano B.E., Clifford C.G., Spalding III C.H., "VAL-II: A New Robot Control System for Automatic Manufacturing", Proceedings of the IEEE Robotics and Automation Conference, Atlanta Georgia, 278-291, March 1985.

[Taylor et al. 83] Taylor R.H., Summers P.D., Meyer J.M., "AML: A Manufacturing Language", The International Journal of Robotics Research,

Vol. 1, No. 3, 19-41, 1982.

[Whitney et al. 84]   Whitney D.E., Lozinski C.A., Rourfe J.M., "Industrial Robot Calibration Method and Results", Proceedings of the ASME Computers in Engineering Conference, Las Vegas, 92-100, August 1984.

[Wu 83]   Wu C.H., "The Kinematic Error Model for the Design of Robot Manipulators", Proceedings of the 1983 American Control Conference, San Francisco, June 1983.

[Yoshikawa 85]   Yoshikawa Tsuneo, "Dynamic Manipulability of Robot Manipulators", Proceedings of the IEEE Robotics and Automation Conference, St. Louis, Missouri, March 1985.

APPENDIX
Effective Drive Train Parameters
for n-Pair Gear Train:
Computation of Effective Compliance K_s.

An n-pair gear drive train may be reduced to fit the drive model used in the previous sections. Consider the gear train model as shown in figure 1 A.

The gear ratio between gear #i and gear #i' is defined as:

$$n_i = \frac{\theta_i}{\theta_i'}$$

If the effective inertia seen at gear, g # i, due to gear, g # i and gear, g # i', is:

$$J_i = J_{gi} + \frac{1}{n_i^2} J_{gi}'$$

Also the effective damping at gear, g # i, shaft is:

$$B_i = B_{gi} + \frac{1}{n_i^2} B_{gi}'$$

Then for any gear pair, as labelled in figure 1. A, the following equations of motion apply:

$$K_{si+1} \left[\frac{1}{n_{i+1}} \theta_{i+1} - \theta_i \right] = J_i \ddot{\theta}_i + B_i \dot{\theta}_i +$$

$$\frac{1}{n_i} K_{si} \left[\frac{1}{n_i} \theta_i - \theta_{i-1} \right]$$

This may be generalized to form the following matrix equation:

$$\mathbf{D}(s)\ \underset{\sim}{\theta}(s) = \underset{\sim}{\tau}(s)$$

where $\mathbf{D}(s) \subset \mathbf{R}^{\ell \times \ell}$ ($\ell = n + 2$) and $\mathbf{D}(s)$ is a tri-diagonal matrix; $\underset{\sim}{\theta}(s) \subset \mathbf{R}^{\ell \times 1}$ is the the vector of angular position of the arm $\theta_a(s)$, the n-gear-pairs, and that of the motor shaft $\theta_m(s)$; $\underset{\sim}{\tau}(s) \subset \mathbf{R}^{\ell \times 1}$ is the torque vector, such that $\underset{\sim}{\tau}(s) = (-\tau_d(s), 0 \ldots 0, \tau_m(s))^t$. The torque $\tau_d(s)$ is the loading torque on the arm and $\tau_m(s)$ is the input motor driving torque. The form of the matrix equation is:

$$
\begin{bmatrix}
G_0(s) & K_0^2 & & & \bigcirc \\
K_1^1 & G_1(s) & K_1^2 & & \\
 & K_j^1 & G_j(s) & K_j^2 & \\
 \bigcirc & & K_{n+1}^1 & G_{n+1}(s)
\end{bmatrix}
\begin{bmatrix}
\theta_a(s) \\
\theta_1(s) \\
\vdots \\
\vdots \\
\theta_n(s) \\
\theta_m(s)
\end{bmatrix}
=
\begin{bmatrix}
-\tau_d(s) \\
0 \\
\vdots \\
\vdots \\
0 \\
\tau_m(s)
\end{bmatrix}
$$
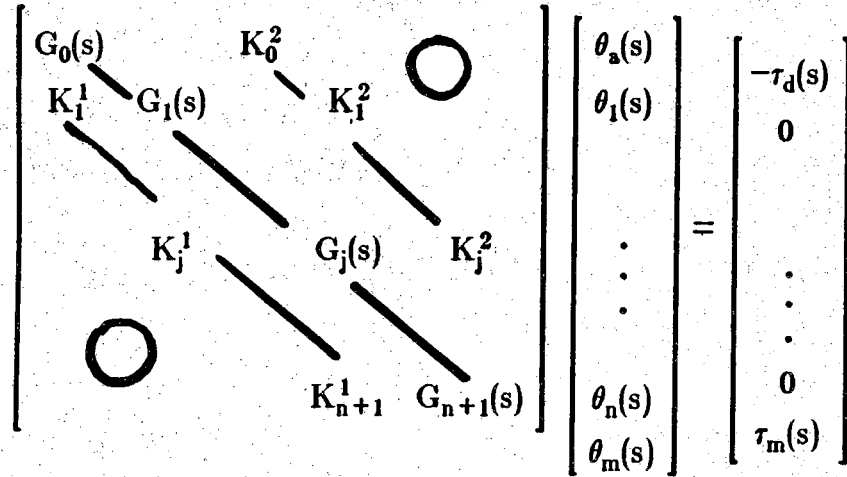
where

$$G_0(s) = J_a s^2 + B_a s + K_{s1}$$

$$K_0^2 = -\frac{K_{s1}}{n_1}$$

The actuator parameters are given by:

$$G_{n+1}(s) = J_m s^2 + B_m s + K_m$$

$$K_{n+1}^1 = K_m$$

and the drive train parameters are given by:

$$K_j^1 = -\frac{1}{n_j} K_{sj} \quad : \quad j = 1 \ldots n$$

$$K_j^2 = -\frac{1}{n_j} K_{sj+1} \quad : \quad j = 1 \ldots (n-1)$$

$$G_j(s) = J_j s^2 + B_j s + \left[\frac{1}{n_j^2} K_{sj} + K_{sj+1} \right] \quad : \quad j = 1 \ldots n$$

$$n_{n+1} = 1$$

$$K_{sn+1} = K_m$$

The effective stiffness K_s of the drive train as seen at the joint output is given as:

$$K_s = 1 \Big/ \left\{ \sum_{i=1}^{m} \frac{1}{K_{si}} \left\{ \prod_{j=1}^{i-1} \frac{1}{n_j^2} \right\} \right\}$$

where, $m = n + 1$, to include the motor shaft stiffness. Notice that the drive shafts at the motor end can be rather compliant in comparison to that of the joint output, if a suitably large gear reduction exists. The analysis, presented here is equivalent to selecting the effective joint stiffness to be that of the most compliant member when scaled appropriately by the gear ratio.
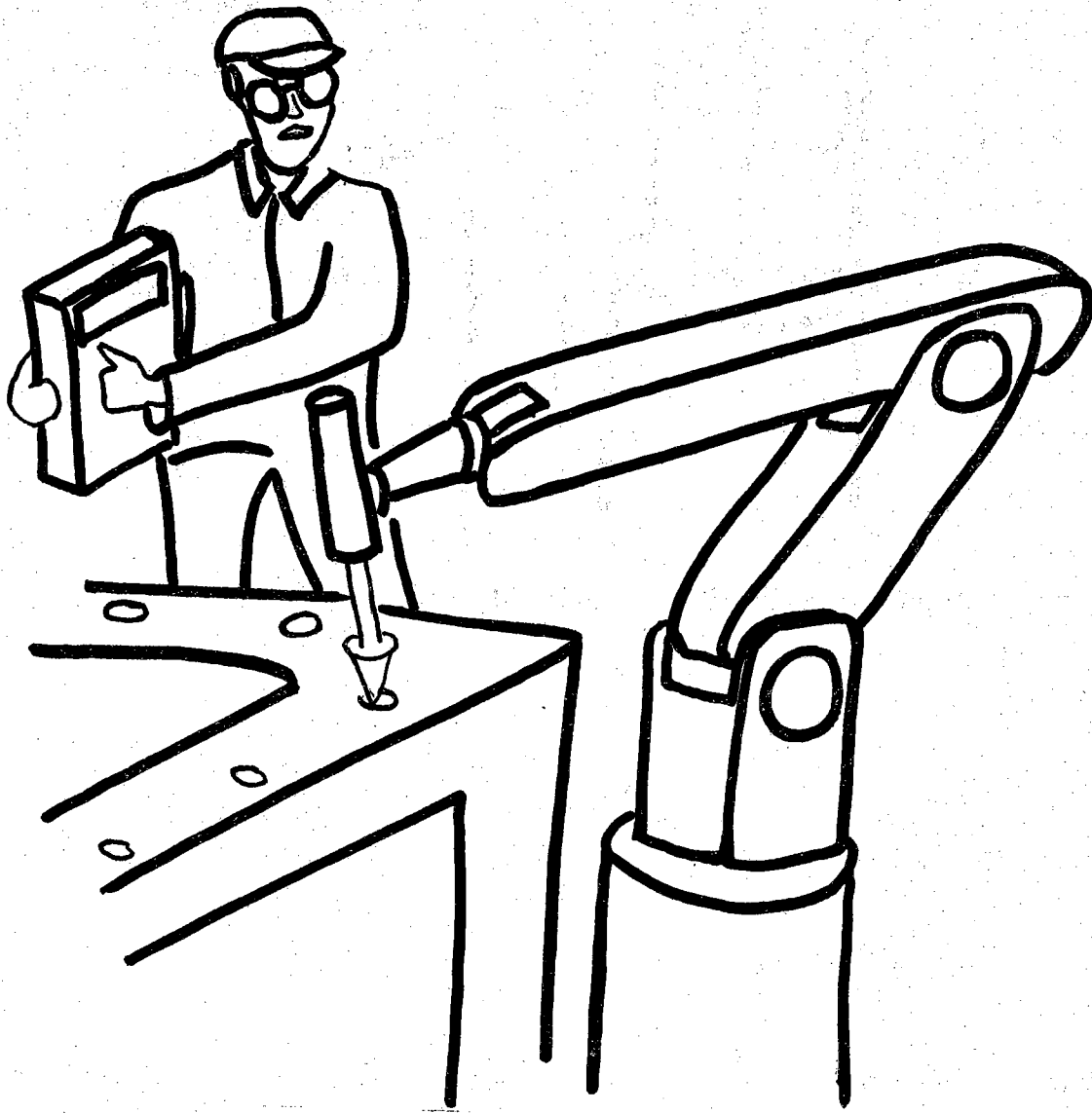
Figure 1.   Robot Programming by "Teach   Play Back Schemes".
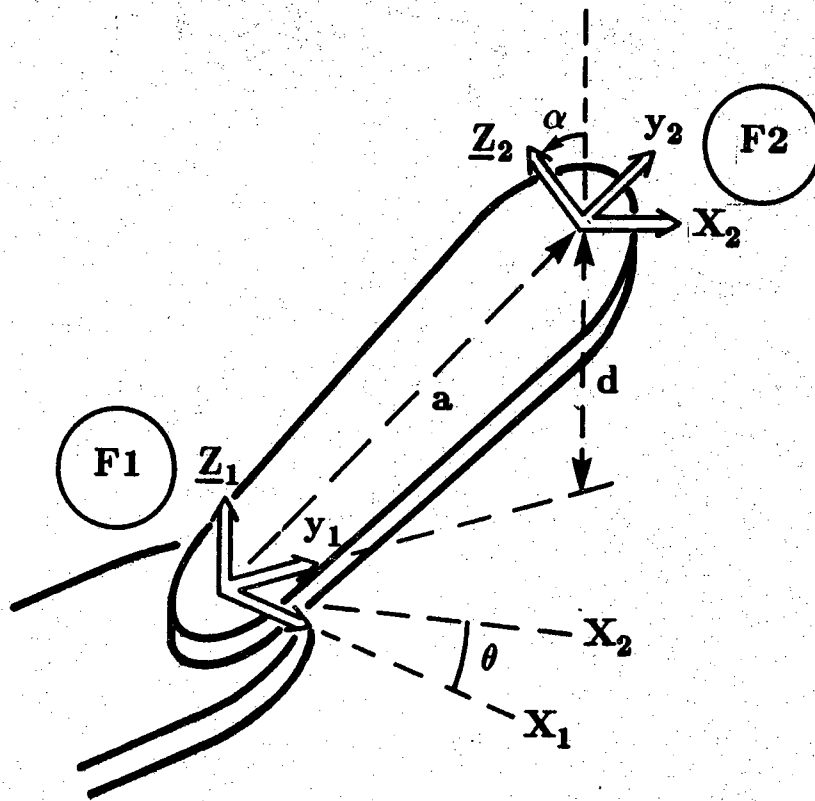
Figure 2. Robot Link Parameters
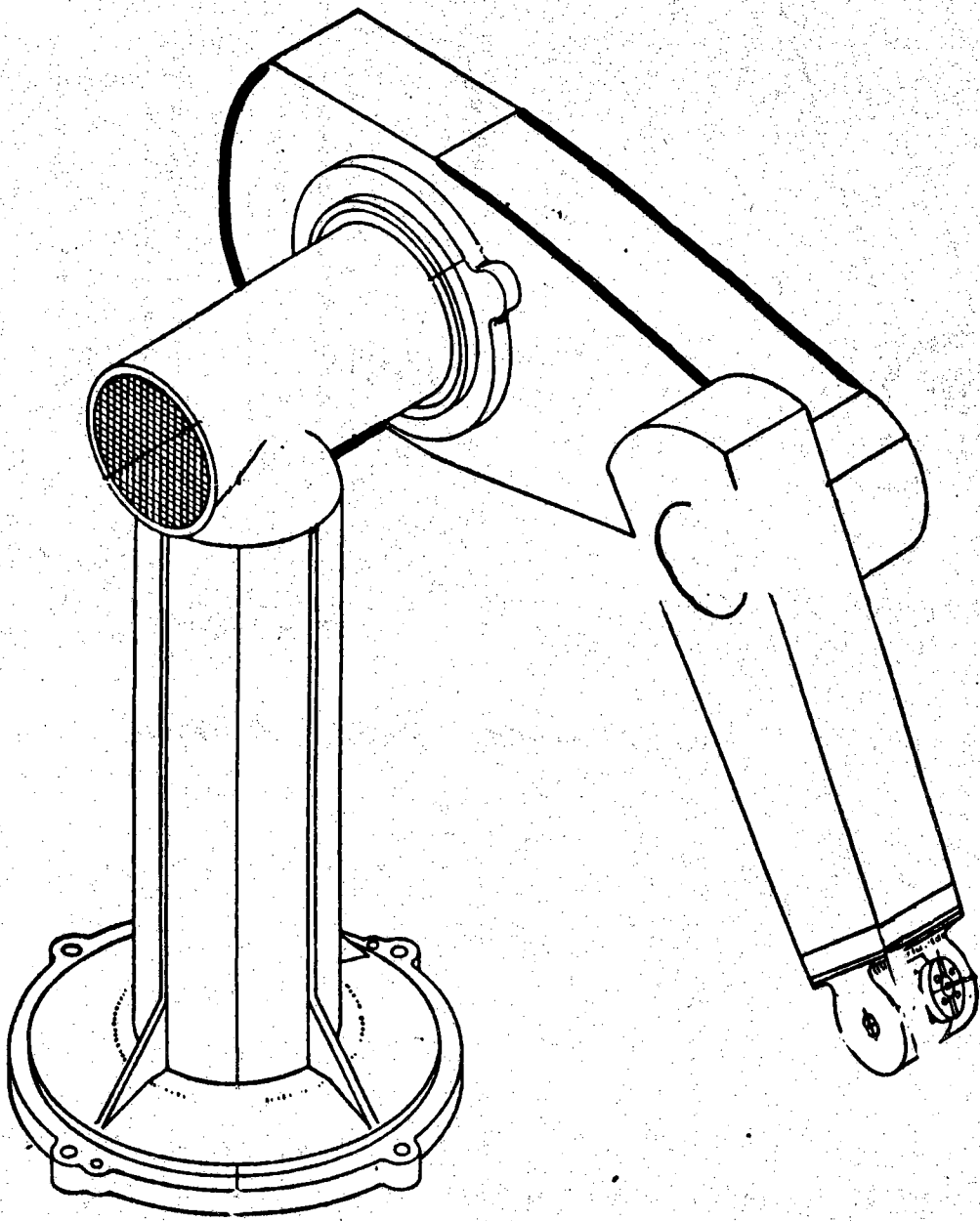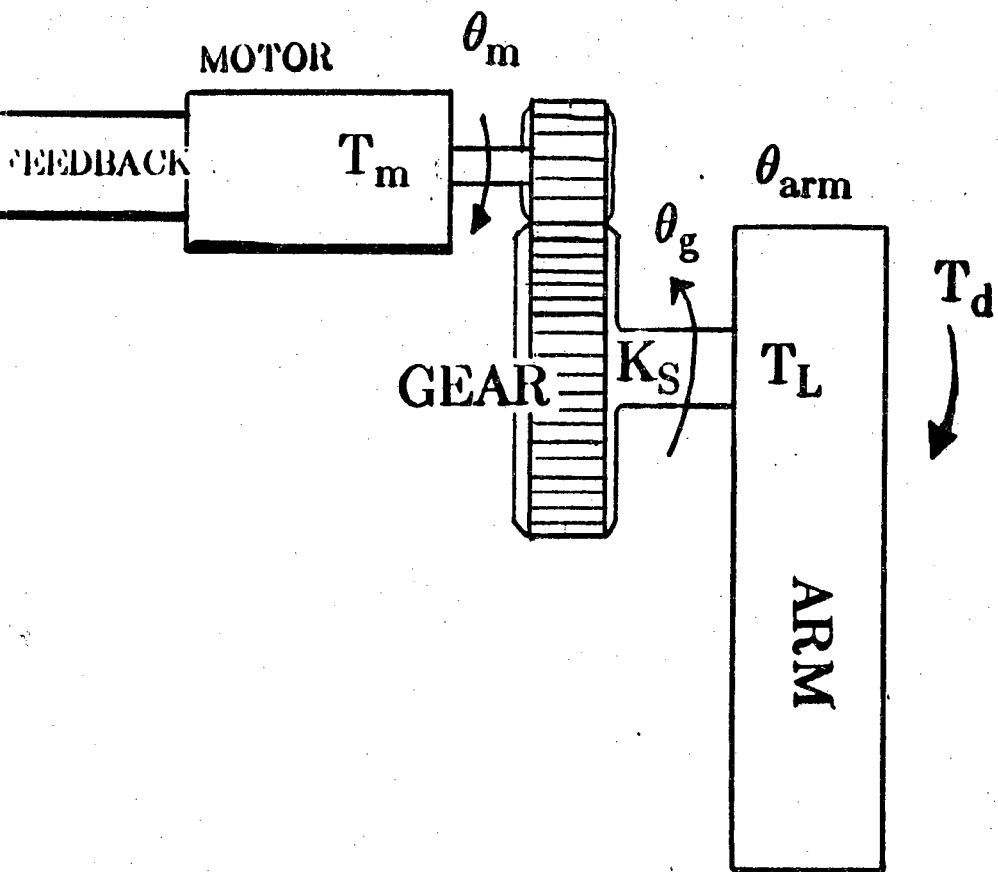
Figure 3.   PUMA   Robot Arm.

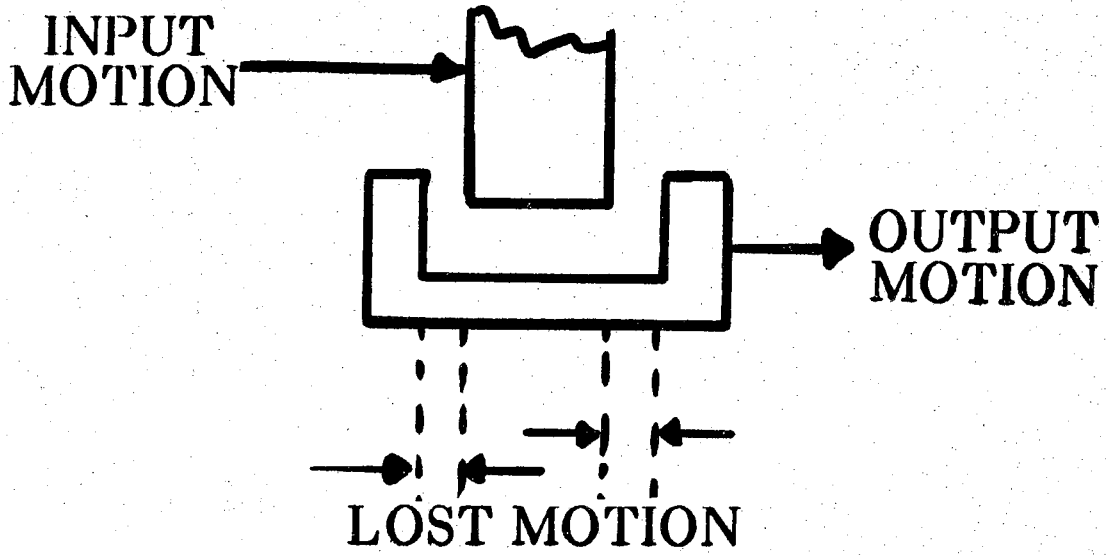Figure 4.   Typical Robot Joint Drive

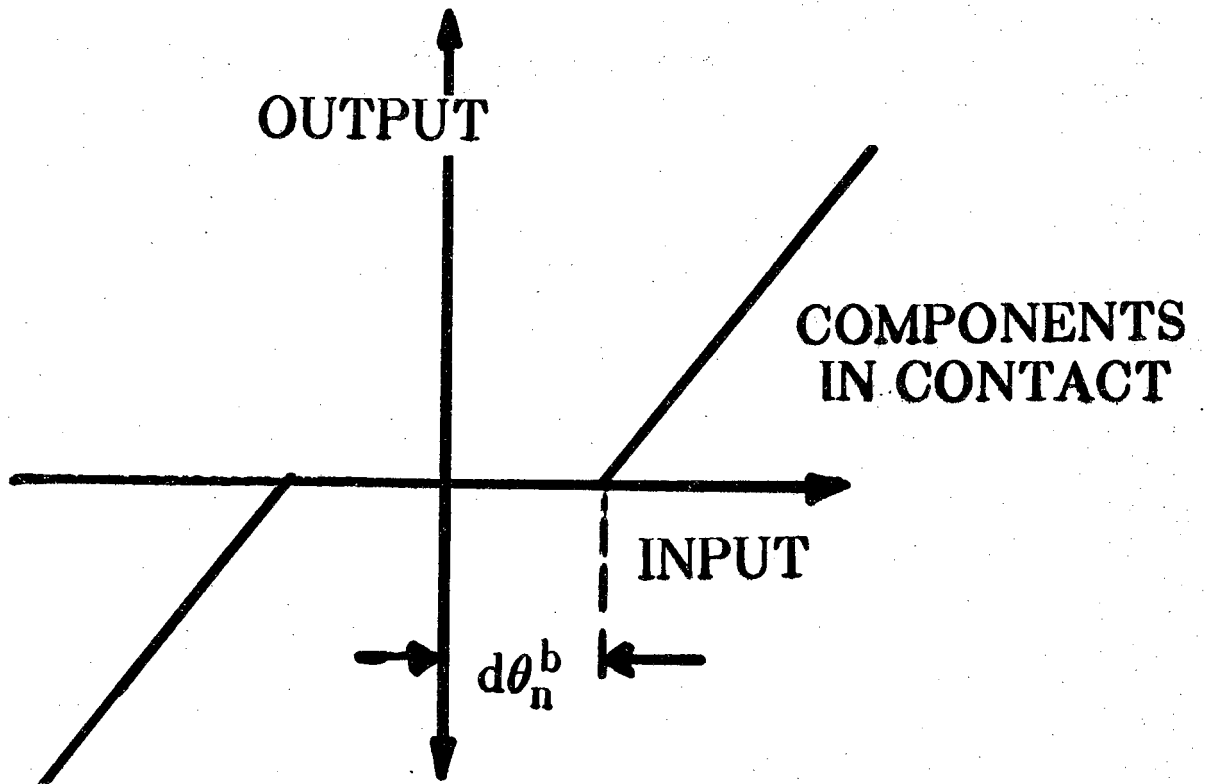Figure 5.   Gear Backlash Gap.

Figure 6.   Input-Output Motion For A Gear Set.
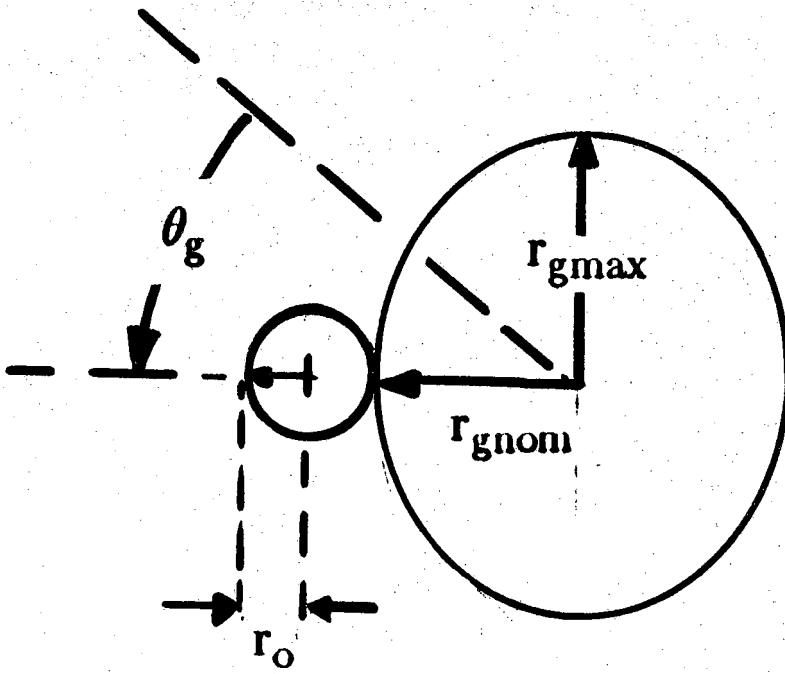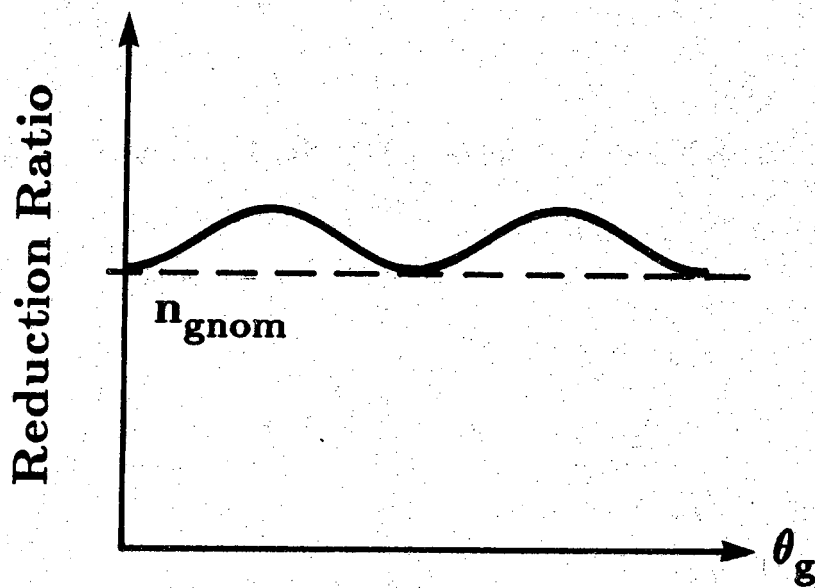
Figure 7.   Gear Eccentricity.

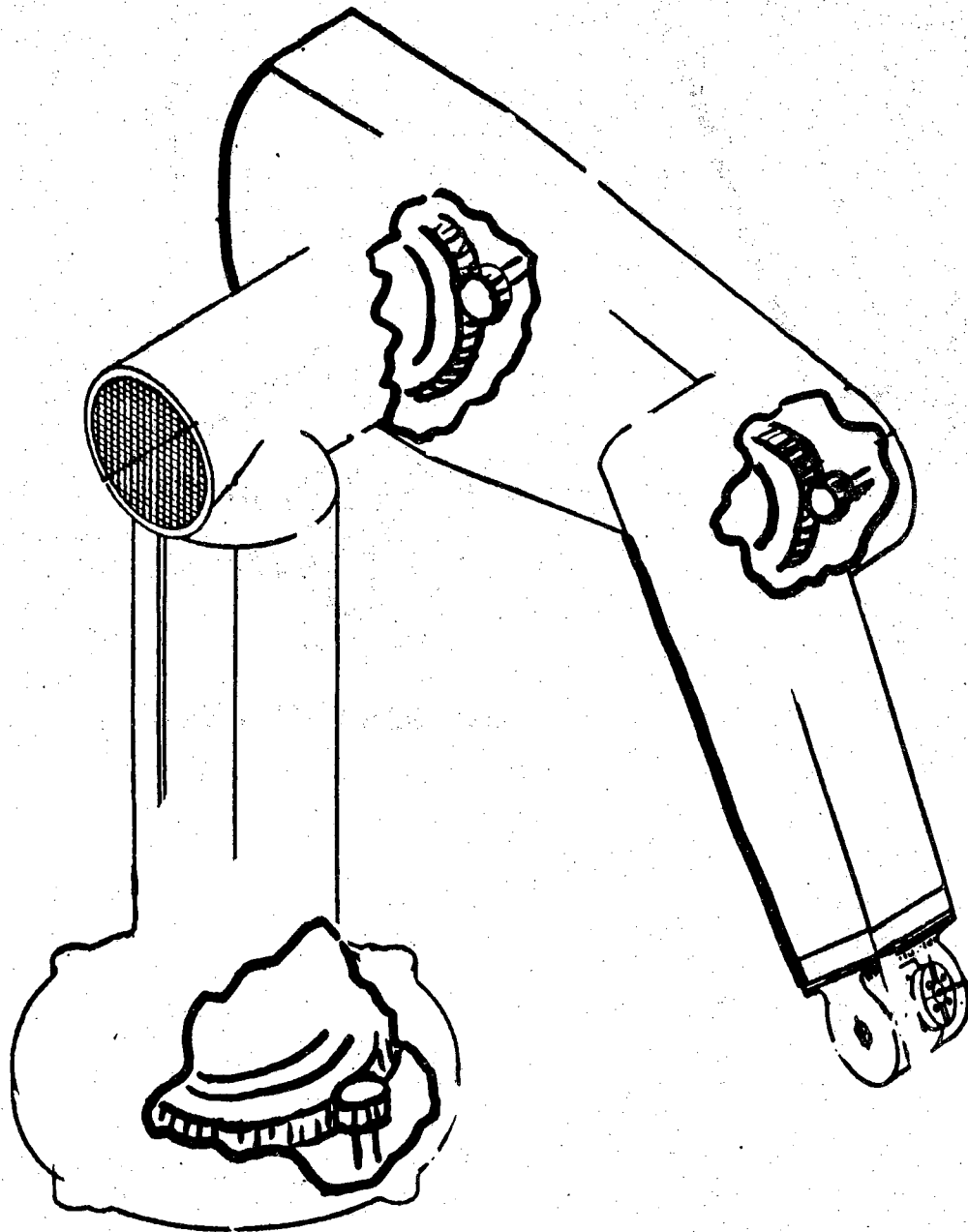Figure 8.   Reduction Ratio Versus Angle θ_g, Due to Gear Eccentricity.
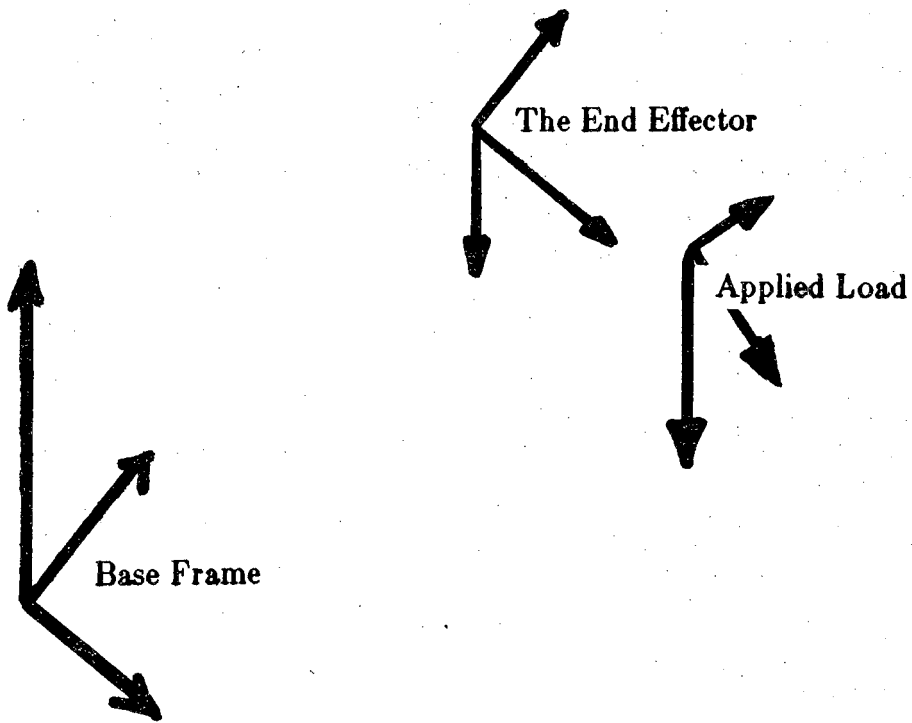
Figure 9.   PUMA Arm Final Joint Drive.

The End Effector

Applied Load

Base Frame

Figure 10.   Applied Load, The End Effector, and Base Frames.
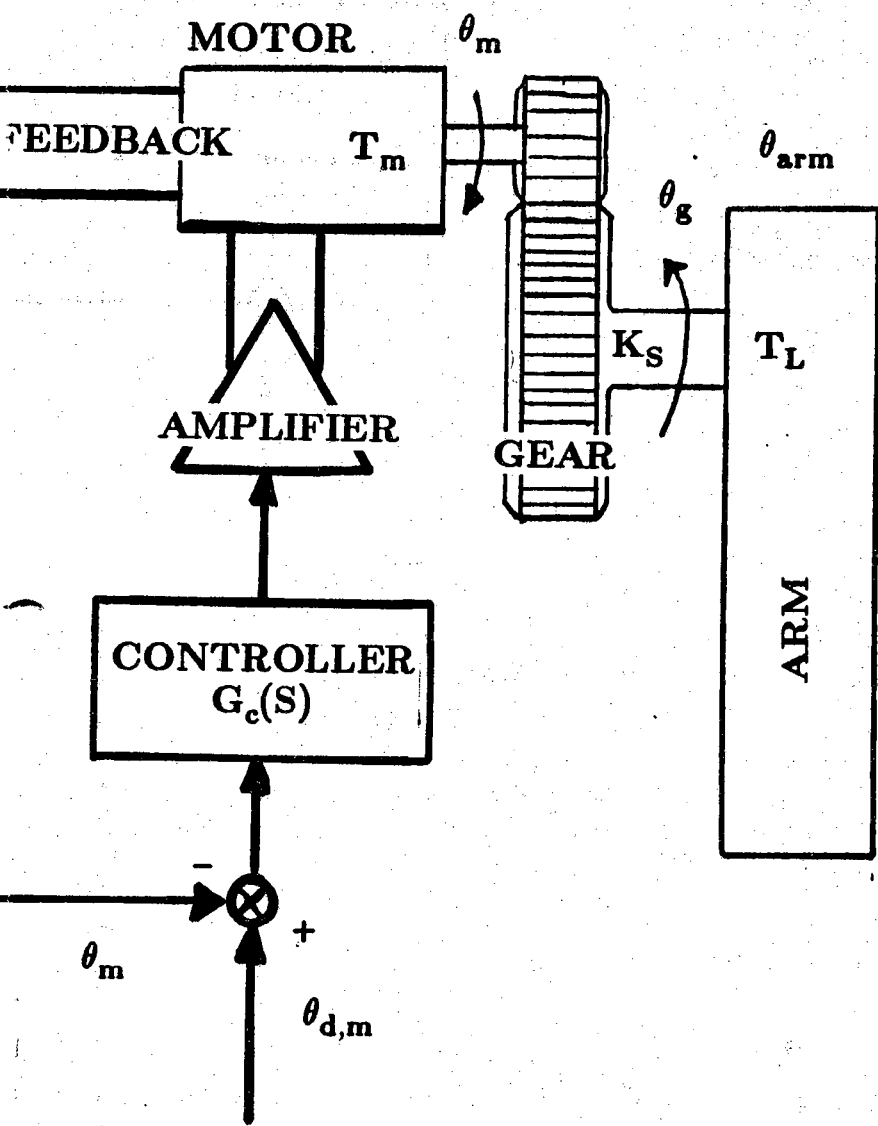
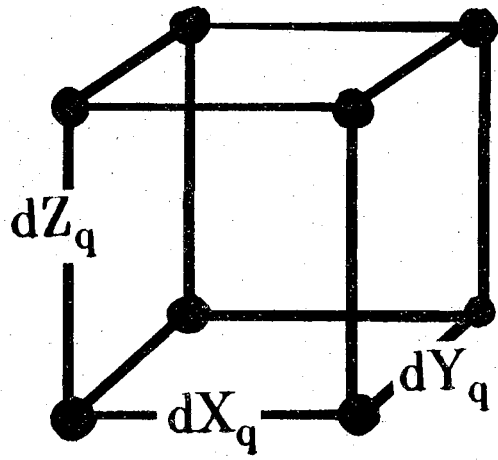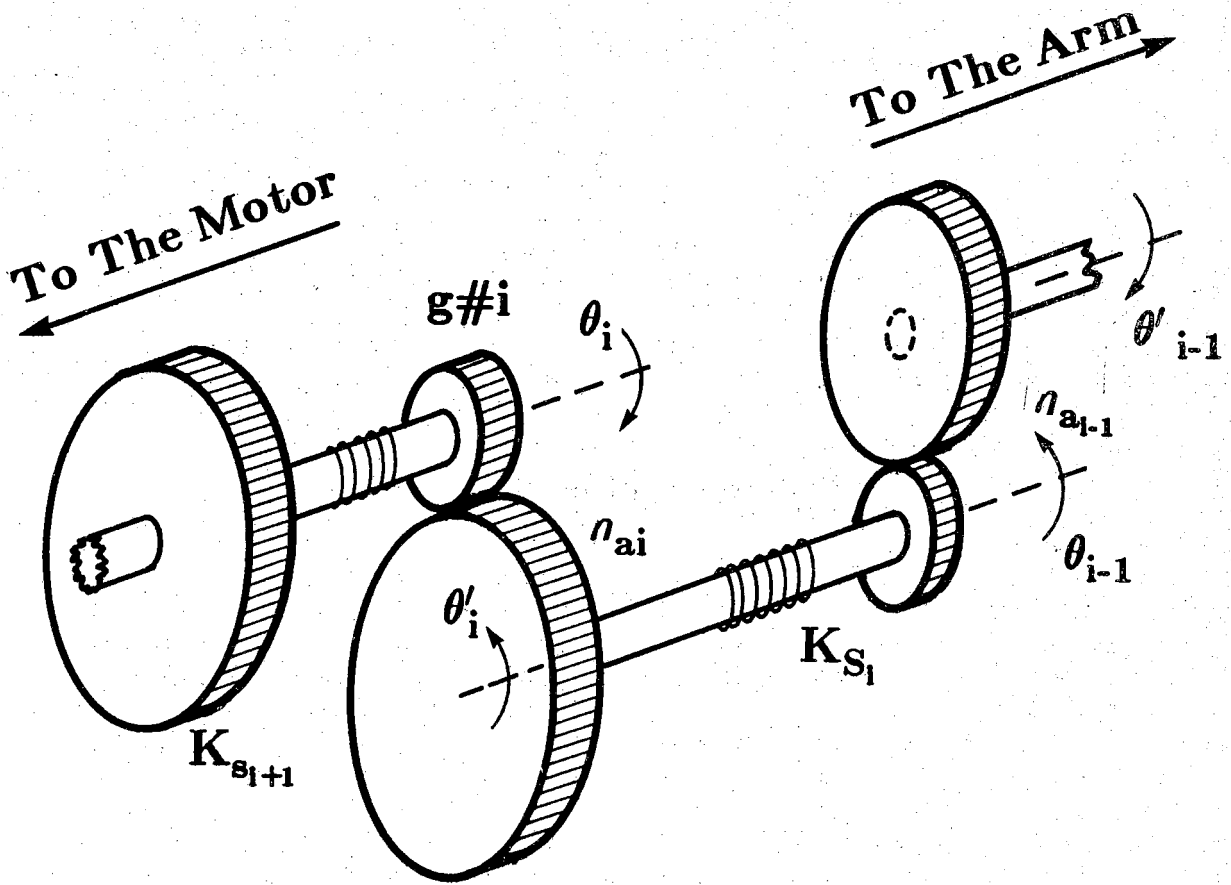Figure 11.   Joint Controller Schematics

Figure 12.   The Quantisation Cube.

Figure A.1.   Realistic Drive Train Model.